Supplementary Information (SI) for Organic Chemistry Frontiers.
This journal is © the Partner Organisations 2024

Impact of boron desymmetrization on supramolecular polymerization of BODIPY dyes

Tobias B. Tischer,[a] Zulema Fernández,[a] Lorenz Borsdorf,[a] Constantin G. Daniliuc,[a] Shigehiro Yamaguchi,[bc] Soichiro Ogi*[b] and Gustavo Fernández*[a]

[a] Universität Münster, Organisch-Chemisches Institut, Corrensstraße 36, 48149 Münster, Germany. E-Mail: fernandg@uni-muenster.de
[b] Department of Chemistry, Graduate School of Science, and Integrated Research Consortium on Chemical Science (IRCCS), Nagoya University, Furo, Chikusa, Nagoya 464-8602, Japan. E-Mail: ogi.soichiro@chem.nagoya-u.ac.jp
[c] Institute of Transformative Bio-Molecules (WPI-ITbM), Nagoya University, Furo, Chikusa, Nagoya 464-8602, Japan

Contents

Experimental Procedures

Materials and Methods

Chemicals and Reagents: All chemicals were purchased from Sigma Aldrich (St. Louis, MO, USA), and BLDpharm (Senefelder ring, Reinbeck, DE) and used without further purification. The used solvents were distilled before usage.

Column chromatography: Preparative column chromatography was performed in self-packed glass columns of different sizes with silica gel (particle size: 40-60 µm, Merck). Solvents were distilled before usage.

NMR spectroscopy: ^{1}H and ^{13}C-NMR spectra were recorded in deuterated solvents at 298 K on DD2 500 and DD2 600 from Agilent. VT-^{1}H-NMR, ^{1}H-^{19}F HOESY and ^{1}H-^{1}H-ROESY measured at different temperatures on DD2 500 and DD2 600 from Agilent as well. Multiplicities for proton signals are abbreviated as s (singlet), d (doublet), t (triplet) and m (multiplet).

Mass spectrometry (MS): Matrix-assisted laser desorption/ionization (MALDI) mass spectra were recorded on a Bruker Daltonics Autoflex Speed using a time of flight (TOF) detector. ESI mass spectra were measured on a Bruker MicrOToF system. The signals are described by their mass/charge ratio (m/z) in u.

UV-Vis spectroscopy: UV-Vis absorption spectra were recorded on a JASCO V-730 with a spectral bandwidth of 1.0 nm and a scan rate of 1000 nm min^{-1}. Glass cuvettes with an optical length of 1 cm and 0.1 mm were used. All measurements were conducted in commercially available solvents of spectroscopic grade.

FT-IR spectroscopy: The measurements were carried out in solution state on a JASCO-FT-IR-4600 equipped with a CaF_2 cell with a path length of 0.1 mm. The temperature was controlled using the pike falcon cell holder.

X-Ray: The crystal structure was measured on a single crystal diffractometer Bruker D8 Venture Photon III system equipped with a micro focus tube Cu ImS (CuKα, $\lambda = 1.54178$ Å) and a MX mirror monochromator. Data were corrected for absorption effects using the multi-scan method (SADABS). The structure was solved and refined using Bruker SHELXTL software package.

Atomic force microscopy (AFM): The AFM images were recorded on a Multimode®8 SPM System manufactured by Bruker AXS. The used cantilevers were NCHV-A by Bruker with a nominal spring constant of 42 N m^{-1}, a nominal frequency of 320 kHz, an average length of 117 µm, an average width of 33 µm and an average tip radius of 8 nm. All samples were spin-coated from freshly prepared solutions onto an HOPG surface.

Synthetic Procedure

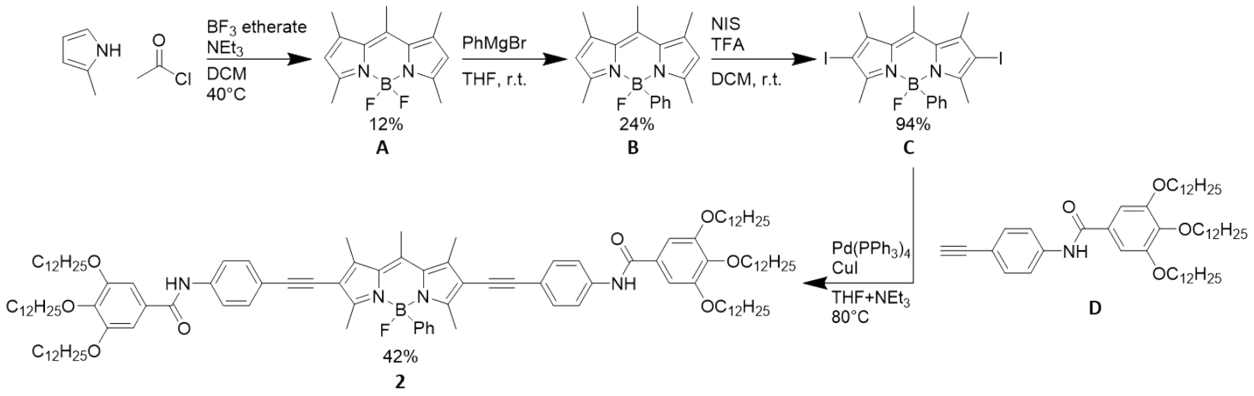

Figure S1: Synthetic route to obtain BODIPY derivative **2**.

Compounds **1**, **A**, and **D** were successfully prepared by following reported synthetic procedures.[1]

Synthesis of BODIPY derivative B[2,3]

The BODIPY dye 4,4-difluoro-1,3,5,7,8-pentamethyl-3a,4-dihydro-4l4-dicyclopenta[b,e]borinine (**A**, 0.0998 g, 0,381 mmol, 1 eq.) was dissolved in dry THF (55 mL) in a dry Schlenk tube. PhMgBr in THF (0.15 mL 3 M, 0.45 mmol, 1.1 eq.) was added to the solution dropwise. The solution was stirred for 30 min at room temperature and subsequently quenched with water. THF was evaporated under reduced pressure and the remaining was extracted with DCM (3 x 25 mL). The combined organic fractions were dried over $MgSO_4$ and the solvent was evaporated under reduced pressure. The crude product was purified by column chromatography (SiO_2), using a gradient of DCM/pentane (from 1/3 to 3:2). The clean product was obtained as an orange solid (29.4 mg, 0.0918 mmol, 24%).

^{1}H NMR ($CDCl_3$, 600 MHz) δ (ppm) = 7.34 (dd, J = 6.2, 1.5 Hz, 2H, CH), 7.18 – 7.10 (m, 3H, CH), 5.96 (s, 2H, CH), 2.68 (s, 3H, CH_3), 2.45, (s, 6H, CH_3), 2.17 (d, J = 1.8 Hz, 6H, CH_3).

^{13}C NMR ($CDCl_3$, 150 MHz) δ (ppm) = 153.80, 141.53, 139.75, 131.99, 131.96, 127.01, 126.17, 121.57, 29.86, 17.66, 16.78, 15.31, 15.28.

HR-MS (APCI): *m/z* 319.17931 [*M*-H]$^-$, calculated for $C_{20}H_{21}BFN_2$: 319.17909.

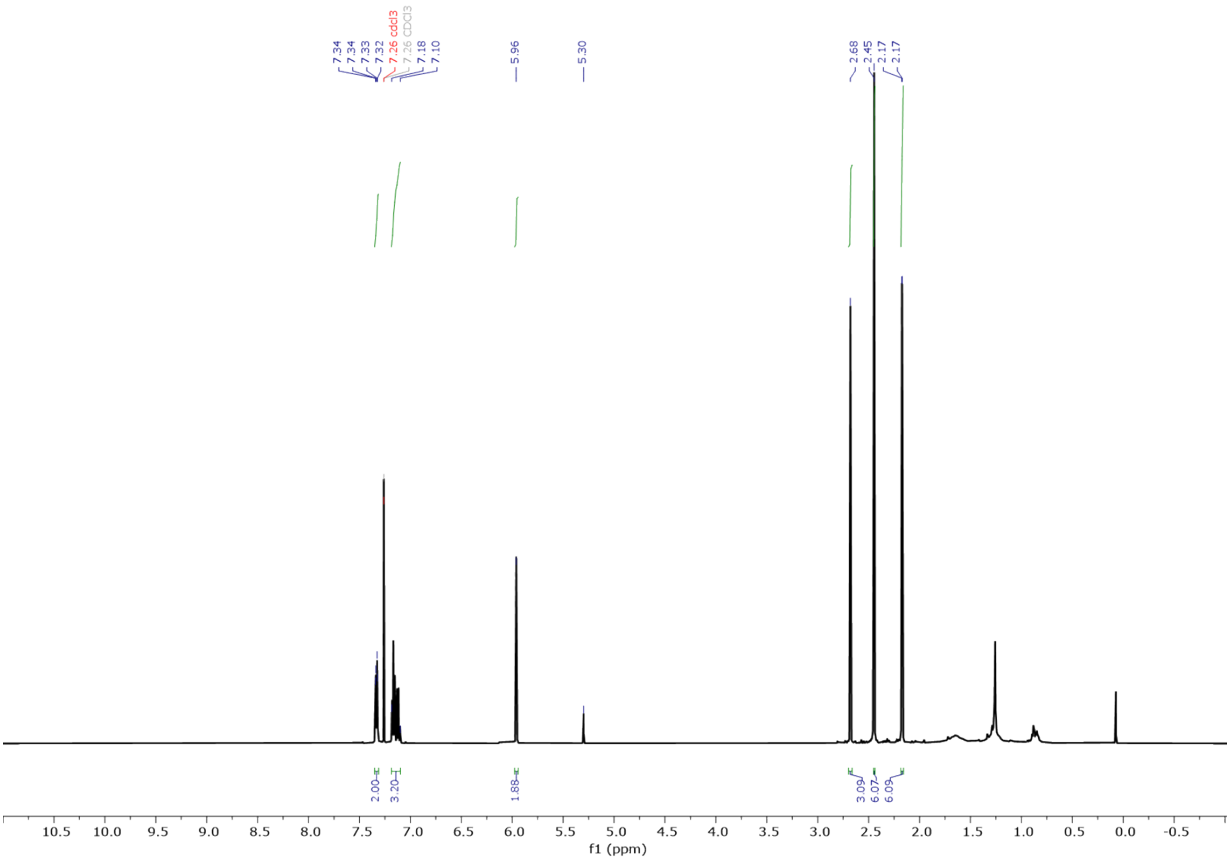

Figure S2: ^{1}H-NMR (600 MHz, $CDCl_3$) of BODIPY derivative **B**.

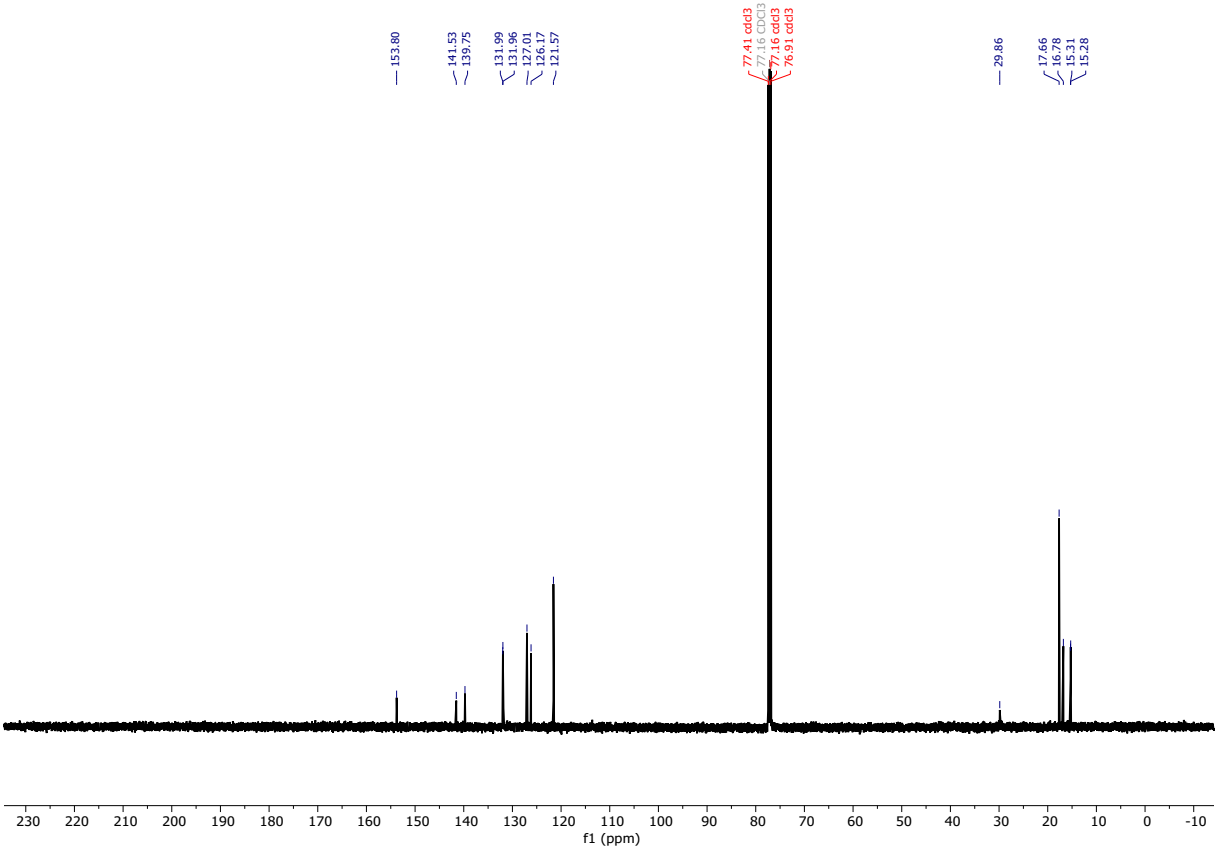

Figure S3: ^{13}C-NMR (150 MHz, $CDCl_3$) of BODIPY derivative **B**.

Synthesis of BODIPY derivative C[4]

The BODIPY dye 4-fluoro-1,3,5,7,8-pentamethyl-4-phenyl-3a,4-dihydro-4l4-dicyclopenta[b,e]borinine (**B**, 0.0351 mg, 0.109 mmol, 1 eq.) was dissolved in DCM (60 mL) and the solution was degassed with Ar. N-Iodsuccinimide (69.8 mg, 0.310 mmol, 2.5 eq.) as well as a catalytic amount of trifluoroacetic acid were added and the reaction mixture was stirred for 20 minutes at room temperature. The solvent was evaporated under reduced pressure and the crude product was purified by column chromatography (SiO_2) using a gradient of DCM/pentane (from 1/1 to 1/0). The pure product was obtained as an orange solid (58.6 mg, 0.102 mmol, 94%).

^{1}H NMR ($CDCl_3$, 600 MHz) δ (ppm) = 7.29 (dd, J = 6.3, 1.6 Hz, 2H, CH), 7.18 – 7.12 (m, 3H, CH), 2.73 (s, 3H, CH_3), 7.50 (s, 6H, CH_3), 7.29 (d, J = 1.8 Hz, 6H, CH_3).

^{13}C NMR ($CDCl_3$, 150 MHz) δ (ppm) = 154.97, 141.84, 141.83, 141.22, 131.91, 131.87, 131.85, 127.25, 126.68, 86.21, 20.19, 18.35, 16.75, 16.72.

HR-MS (APCI): *m/z* 570.97125 $[M-H]^-$, calculated for $C_{20}H_{19}BFI_2N_2$: 570.97238.

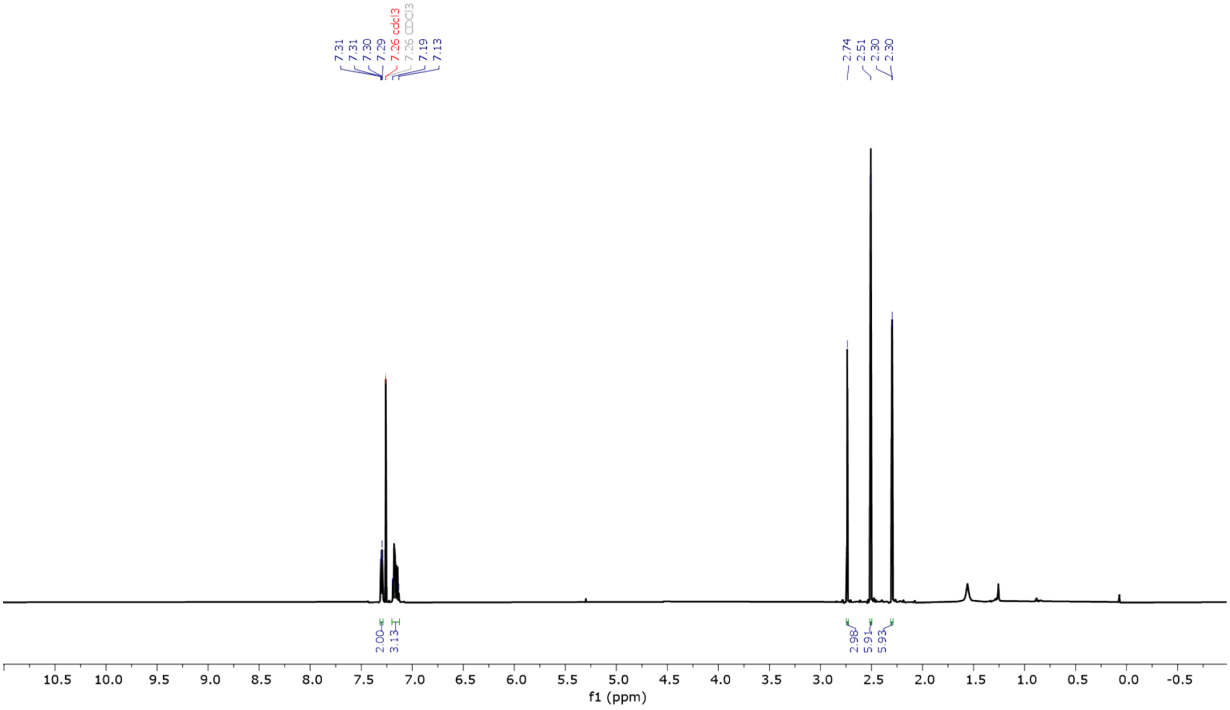

Figure S4: ^{1}H-NMR (600 MHz, $CDCl_3$) of BODIPY derivative **C**.

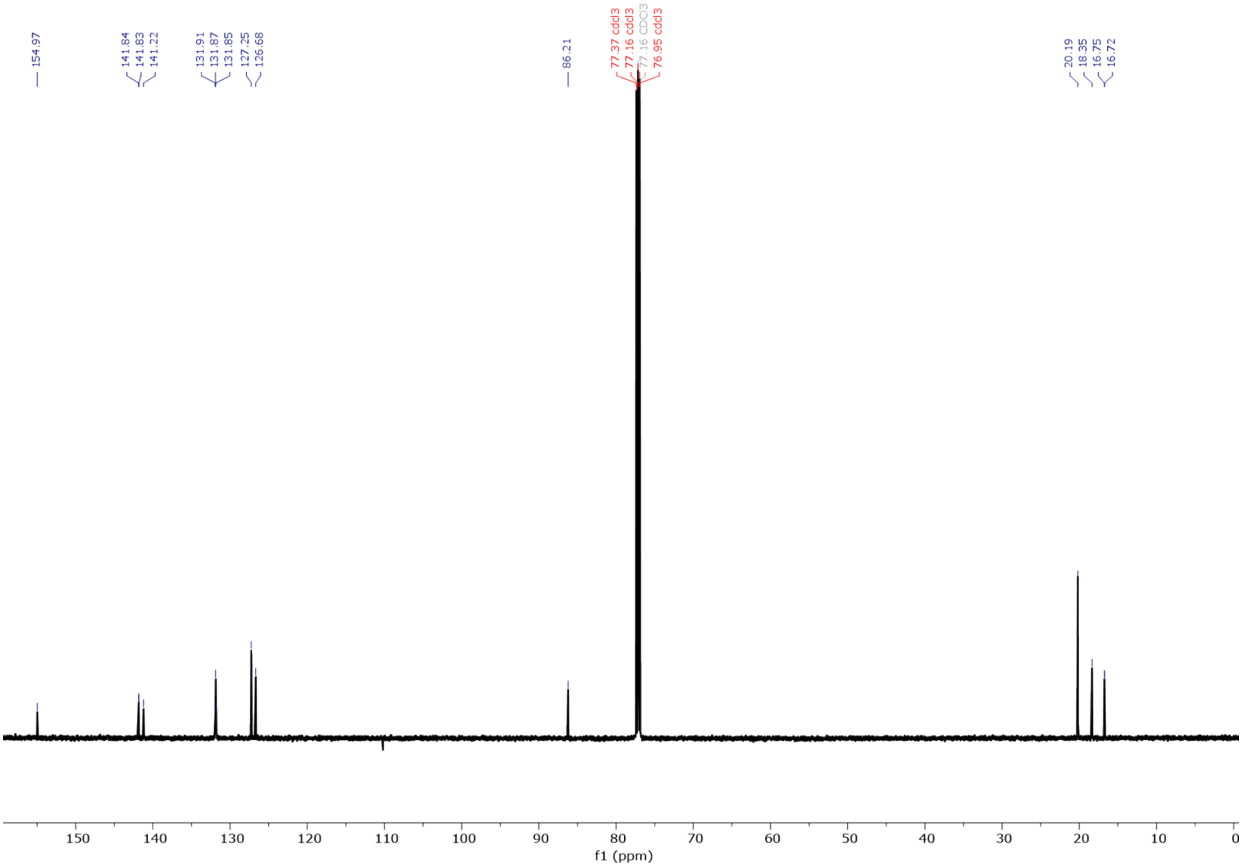

Figure S5: ^{13}C-NMR (150 MHz, $CDCl_3$) of BODIPY derivative **C**.

Synthesis of BODIPY derivative 2[1]

The BODIPY dye 4-fluoro-2,6-diiodo-1,3,5,7,8-pentamethyl-4-phenyl-3a,4-dihydro-4l4-dicyclopenta[b,e]borinine (**C**, 50.6 mg, 0.0885 mmol, 1 eq.), 3,4,5-tris(dodecyloxy)-N-(4-ethynylphenyl)benzamide (**D**, 150 mg, 0.194 mmol, 2.2 eq.), $Pd(PPh_3)_4$ (10.3 mg, 0.0089 mmol, 0.1 eq) and CuI (11 mg, 0.0058 mmol, 0.05 eq) were dissolved in a mixture of dry and degassed THF (4 mL) and NEt_3 (1 mL). The reaction mixture was heated to 80 °C and stirred overnight. After the reaction cooled down to room temperature, the solvent was evaporated under reduced pressure and the crude product was purified by column chromatography (SiO_2) using a gradient of cyclohexane/ethyl acetate (from 100/1 to 100/9) as an eluent. The pure product was obtained as a purple solid (65.9 mg, 0.0372 mmol, 42%).

^{1}H NMR (CD_2Cl_2, 600 MHz) δ (ppm) = 7.98 (s, 2H, NH), 7.62 (d, J = 8.6 Hz, 4H, CH), 7.45 (d, J = 8.6 Hz, 4H, CH), 7.33 (d, J = 6.6 Hz, 2H, CH), 7.20–7.13 (m, 3H, CH), 7.04 (s, 4H, CH), 4.00 (m, 12H, CH_2), 2.78 (s, 3H, CH_3), 2.62 (s, 6H, CH_3), 2.35 (s, 6H, CH_3), 1.83 – 1.70 (m, 12H, CH_2), 1.50 – 1.44 (m, 12H, CH_2), 1.38 – 1.28 (m, 96 H, CH_2), 0.88 (t, J = 6.8 Hz 18H, CH_3).

^{13}C NMR (CD_2Cl_2, 150 MHz) δ (ppm) = 165.81, 156.71, 153.66, 143.41, 141.83, 141.31, 138.52, 132.31, 132.22, 130.05, 128.88, 127.44, 126.91, 120.28, 119.60, 116.33, 105.96, 96.47, 82.1, 73.89, 69.77, 32.38, 32.37, 30.78, 30.20, 30.19, 30.18, 30.15, 30.14, 30.11, 30.09, 30.03, 29.87, 29.83, 29.81, 26.54, 26.53, 23.13, 23.12, 17.61, 16.47, 14.40, 14.37, 14.30.

HR-MS (APCI): *m/z* 1863.41679 $[M-H]^-$, calculated for $C_{122}H_{184}BFN_4O_8$: 1863.41619.

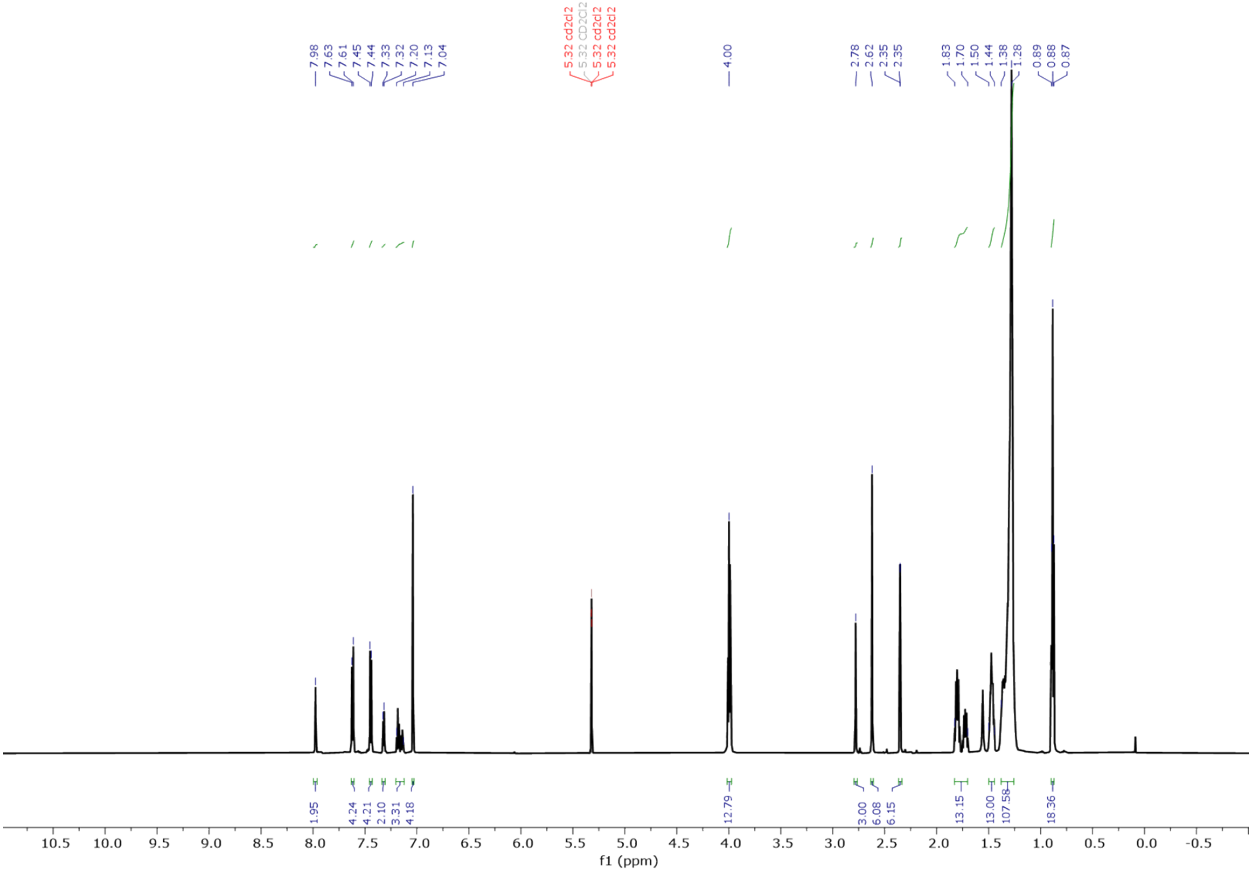

Figure S6: ^{1}H-NMR (600 MHz, CD_2Cl_2) of BODIPY derivative **2**.

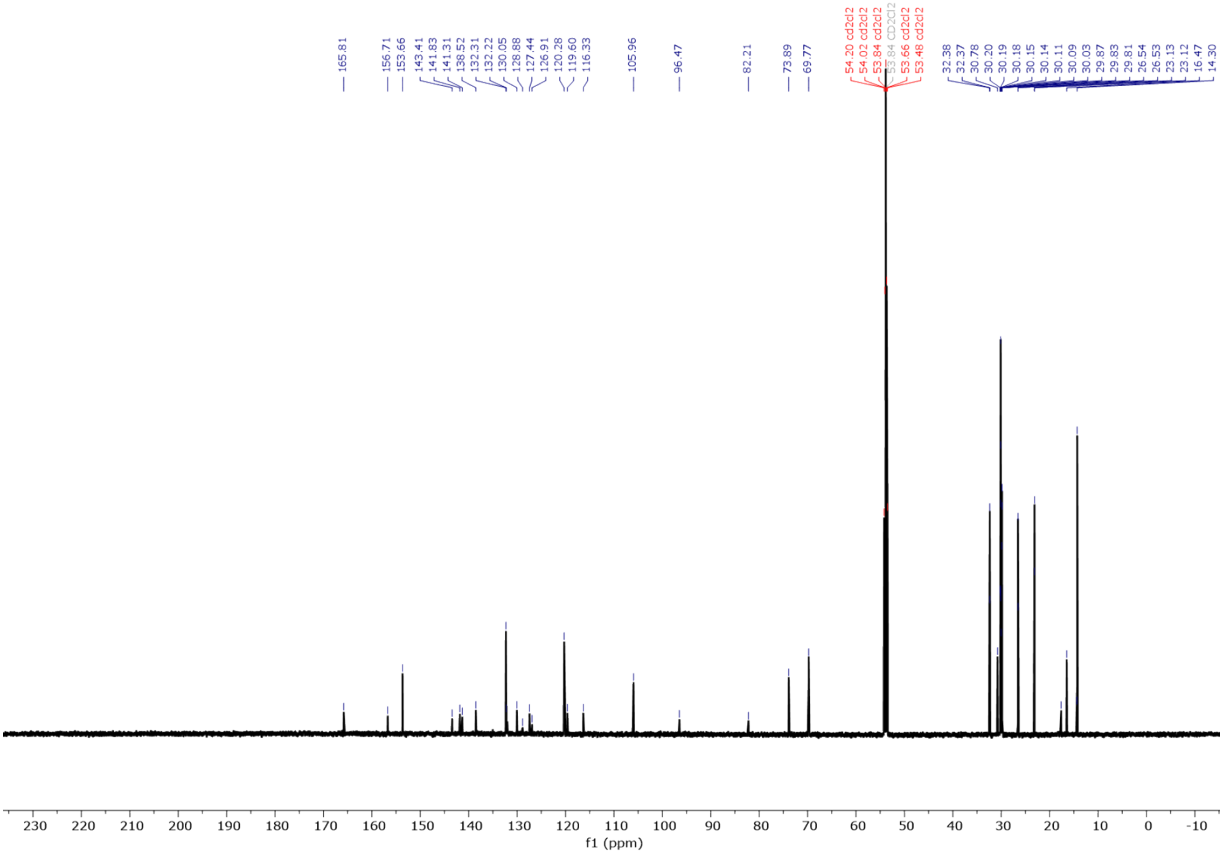

Figure S7: ^{13}C-NMR (150 MHz, CD_2Cl_2) of BODIPY derivative **2**.

Results and Discussion

Supplementary Figures

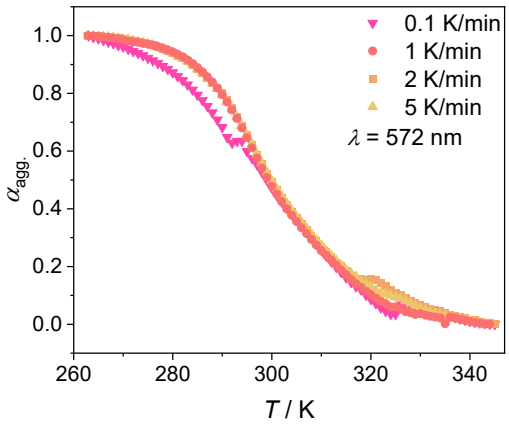

Figure S8: Plot of degree of aggregation *vs*. temperature, derived from different UV-vis cooling experiments of **2** using different cooling rates (MCH, 10 µM, 572 nm).

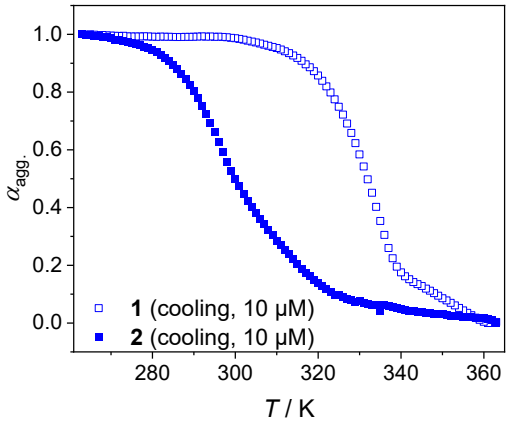

Figure S9: Plot of degree of aggregation ($\alpha_{agg.}$) *vs*. temperature, derived from UV-vis cooling experiments of **1** (MCH, 1 K/min, 10 µM, 572 nm) and **2** (MCH, 1 K/min, 10 µM, 577 nm). The data show that the aggregation of **2** starts at lower temperatures.

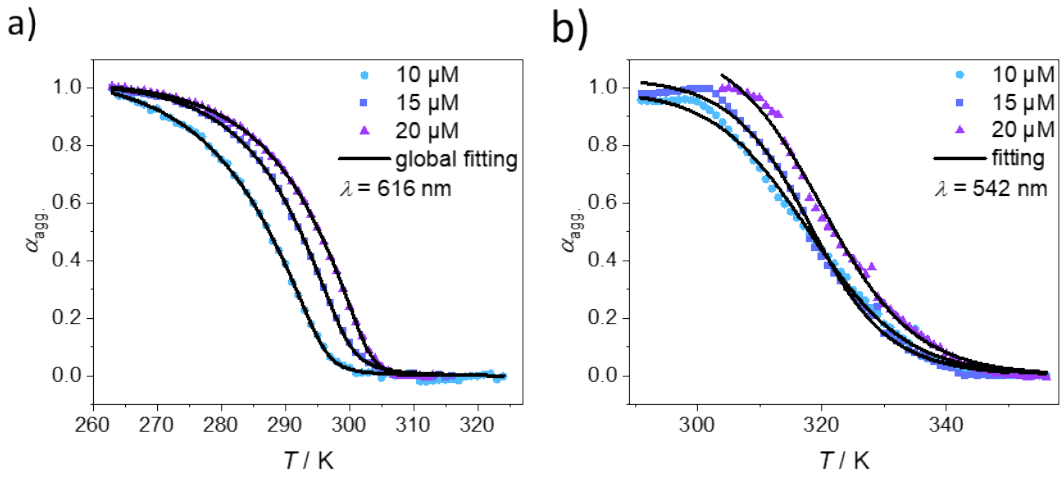

Figure S10: cooling curves of **2** at different concentrations (MCH, 1 K/min, 616 nm) that indicate the presence of a cooperative effect in the transformation from **2-I** to **2-H**, fitted by the nucleation-elongation model[5] (a). b) cooling curves describing the transformation from monomer to **2-I** (MCH, 1 K/min, 542 nm). The fits to the nucleation-elongation model are unable to reproduce the experimental data, particularly at low temperatures. This can be explained by the impossibility to isolate the formation of **2-I** from the transformation to **2-H** at any wavelength.

Table S1: Thermodynamic parameters for the formation of **2-H** from cooling experiment (MCH, 1 K/min), obtained upon globally fitting the cooling curves shown in Figure S10a to the nucleation-elongation model.

ΔH^0_{nucl} / kJ mol^{-1}	ΔH^0 / kJ mol^{-1}	ΔS^0 / kJ mol^{-1} K^{-1}	T_e[a] / K	K_{nucl} / M^{-1}	K_{el} / M^{-1}	σ
-13.4 ± 0.3	-68.7 ± 0.7	-0.138 ± 0.003	294.3, 298.6, 301.7	3.05×10^2	6.82×10^4	0.0045

[a] c = 10, 15, 20 µM

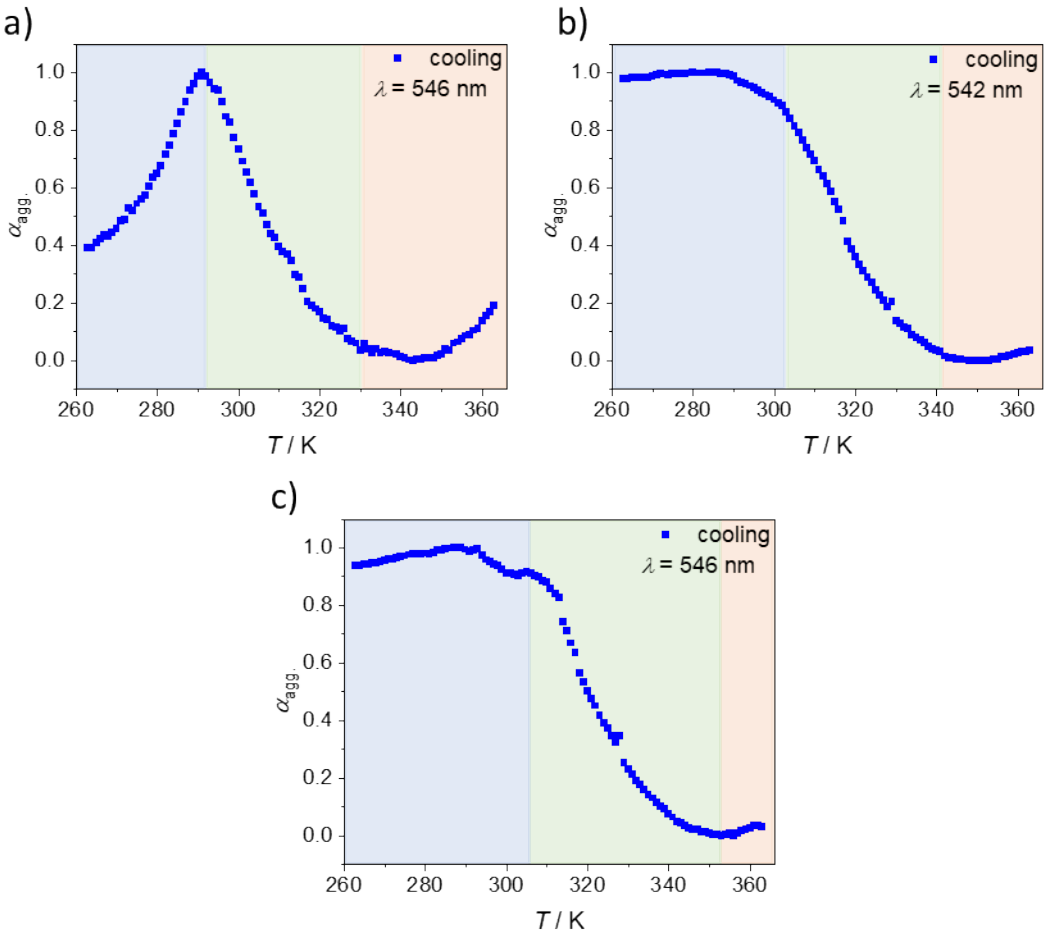

Figure S11: Cooling curves at a) 5 µM, b) 15 µM and c) 20 µM (MCH, 1 K/min) to construct the phase diagram of **2** shown in Figure 2e.

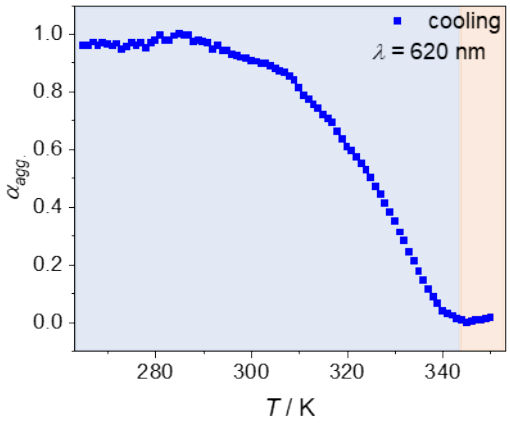

Figure S12: Cooling curve of **1** (MCH, 10 µM, 1 K/min, 620 nm) showing only a single step self-assembly process.

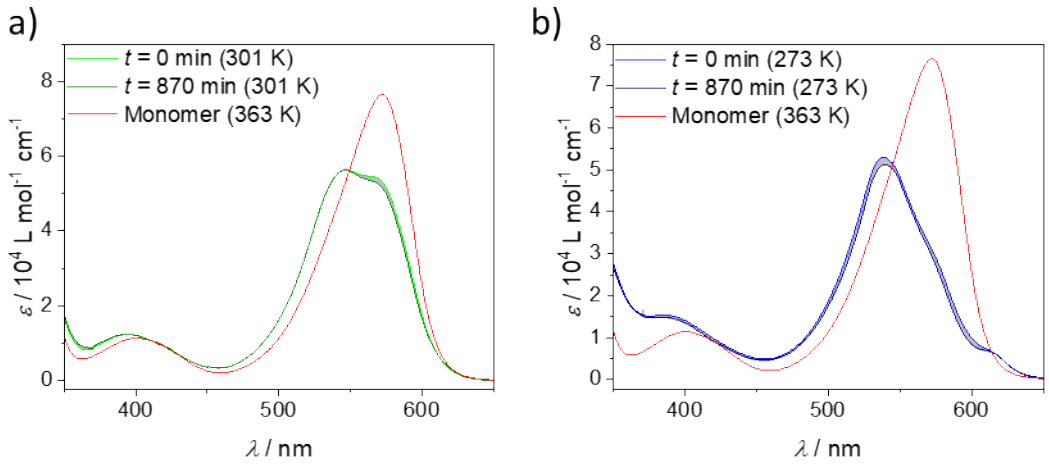

Figure S13: Time-dependent studies of **2** (10 µM, MCH) at 301 K (a) and 273 K (b) to show the stability of the different species.

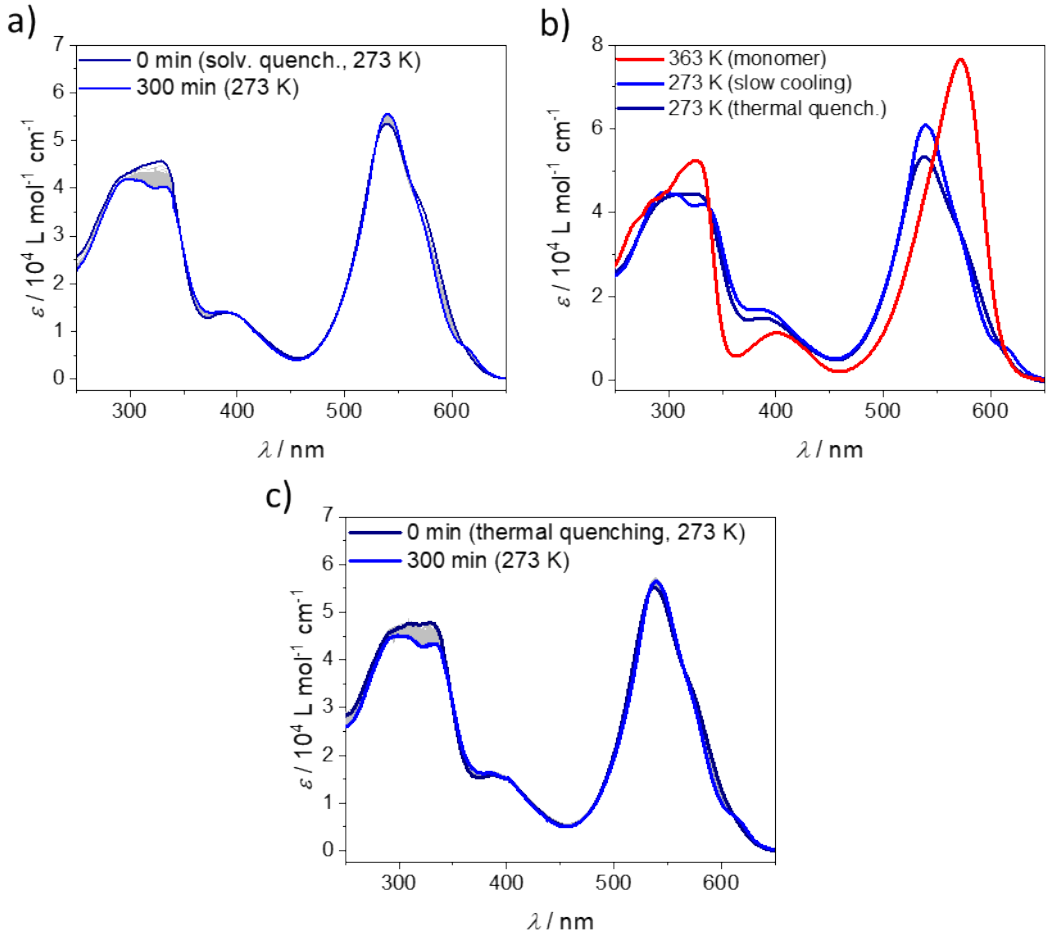

Figure S14: a) time-dependent UV-Vis experiment after solvophobic quenching of **2** (10 µM, 273 K, 100 µL $CHCl_3$, 3900 µL MCH). b) UV/Vis experiment of **2** after equilibrating a solution (MCH, 10 µM) at 363 K for 15 min. and quenching it in an ice bath for 1 min. c) shows the corresponding time-dependent development (MCH, 273 K) of the thermal quenching experiment.

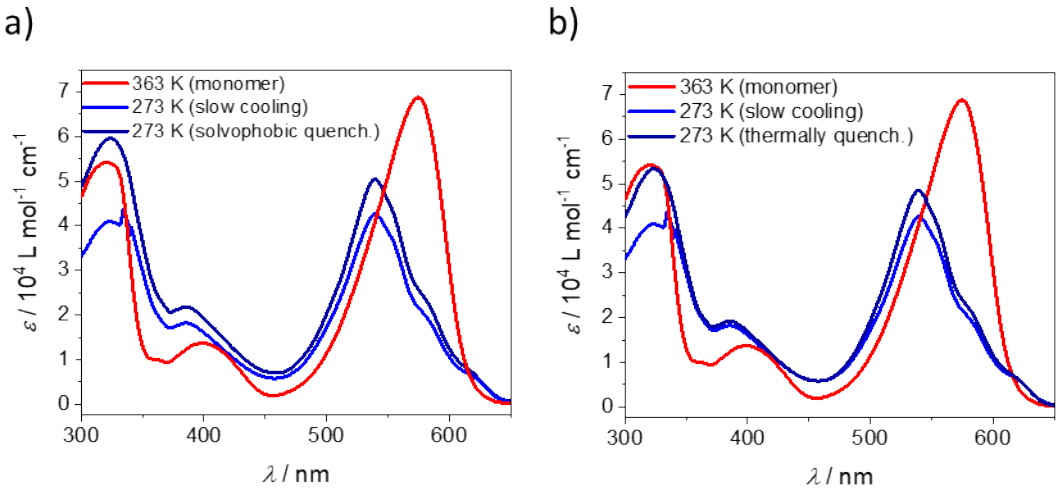

Figure S15: Solvophobic (a) and thermal (b) quenching experiments of **1** (MCH, 10 µM,273 K).

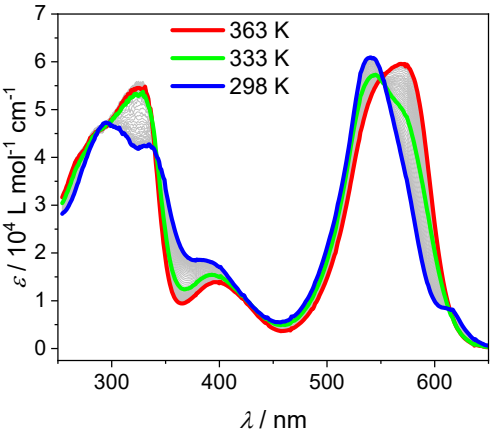

Figure S16: VT UV-Vis experiment of **2** to investigate the presence of **2-I** at high concentrations (0.5 mM, MCH, 1 K/min).

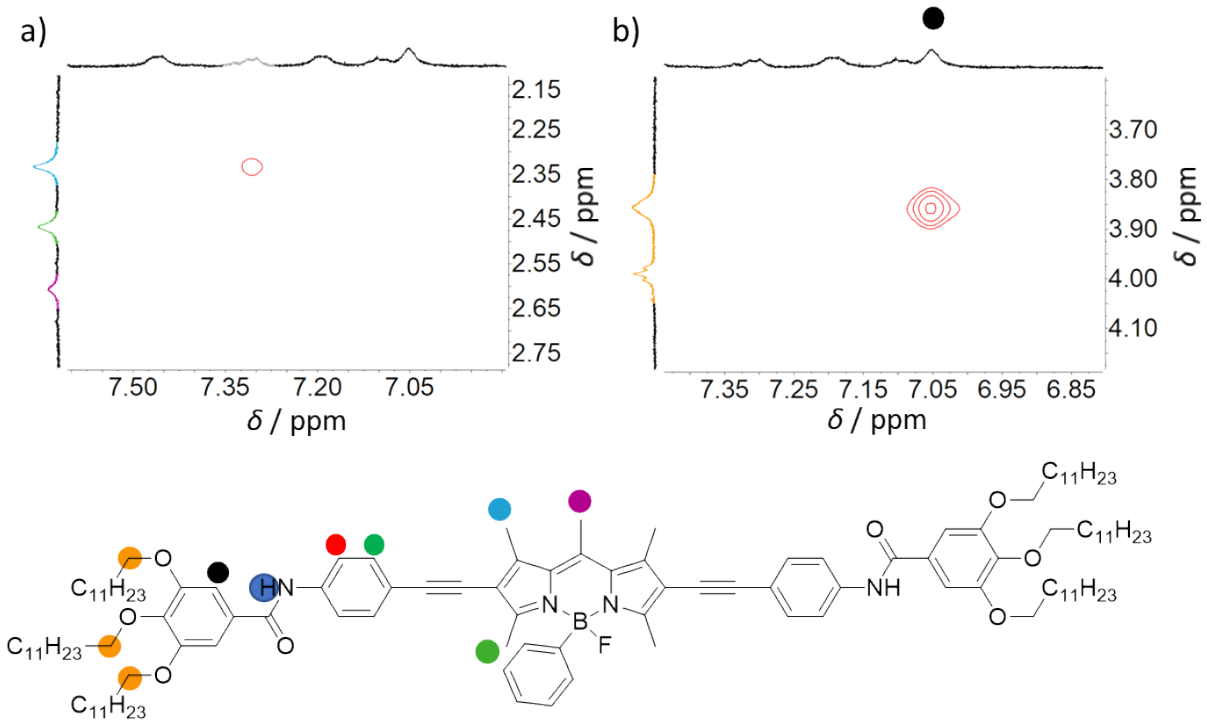

Figure S17: Partial ^{1}H-^{1}H ROESY NMR of **2-H** highlighting the relevant correlation signals (1 mM, 333 K, MCH-d_{14}).

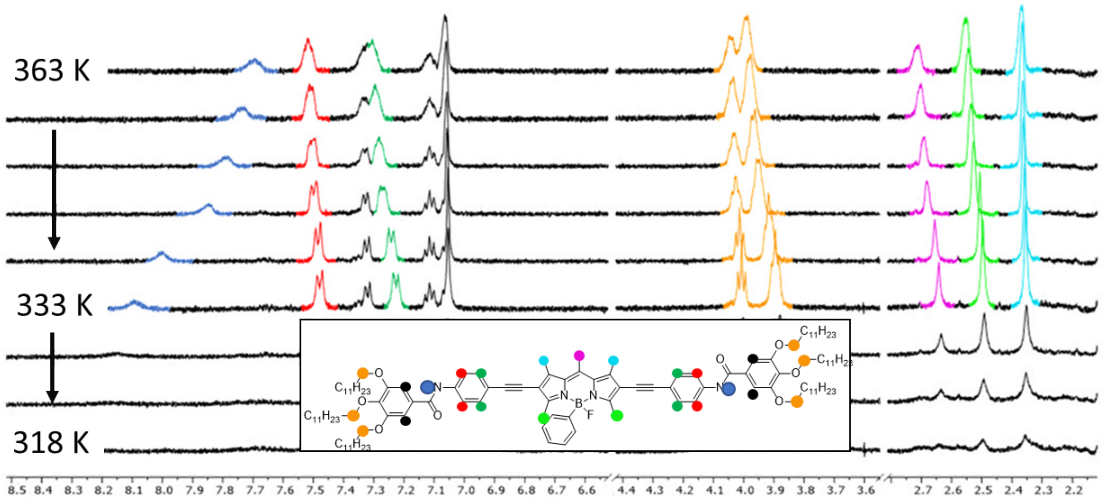

Figure S18: VT ^{1}H-NMR of **2** (0.5 mM, MCH-d_{14}) from 363 K to 293 K. The NMR shows similar characteristics compared to the higher concentrated solution of **2**.

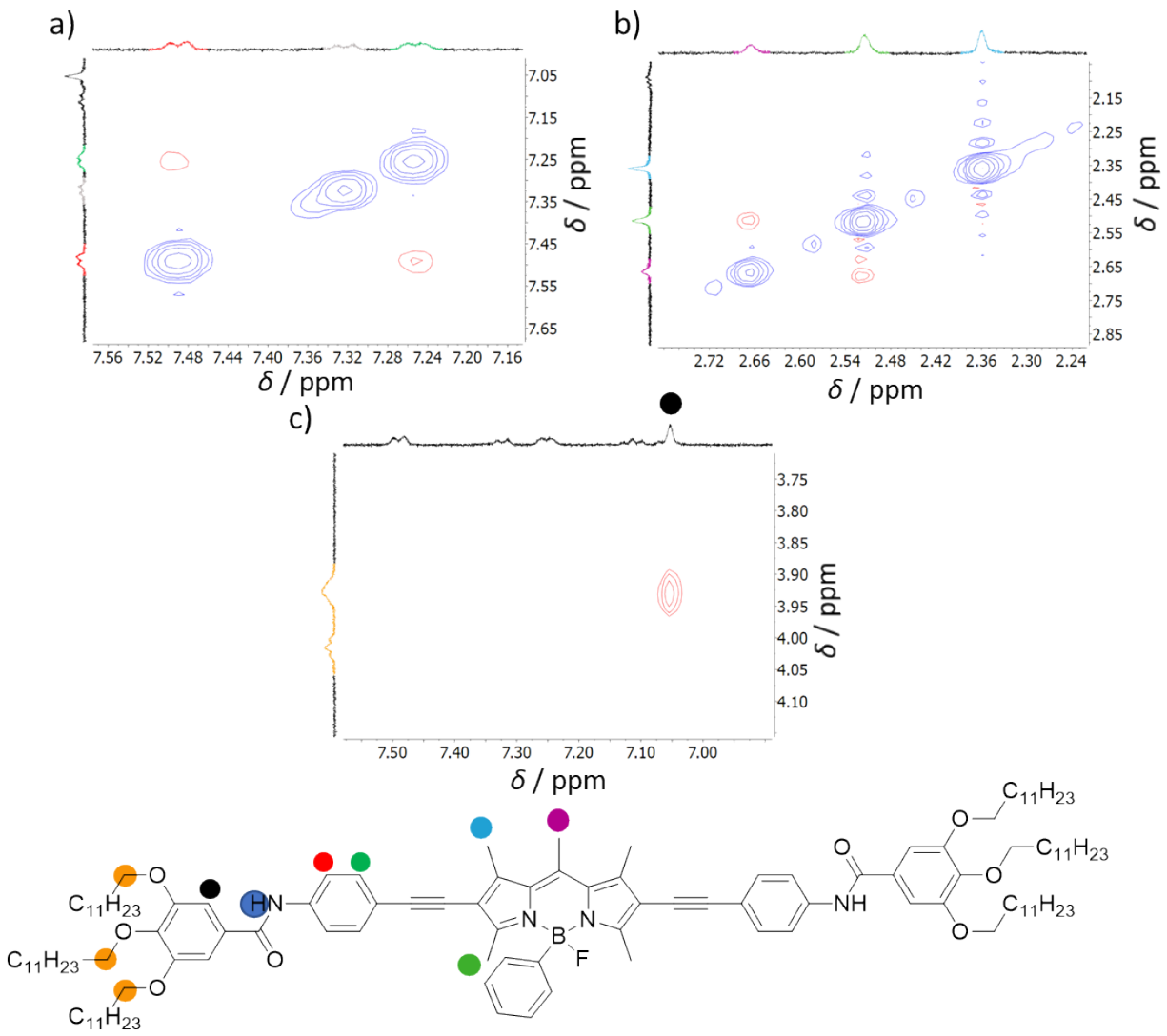

Figure S19: Partial 2D ROESY experiments of **2** (0.5 mM, MCH-d_{14}, 338 K).

Morphological Studies

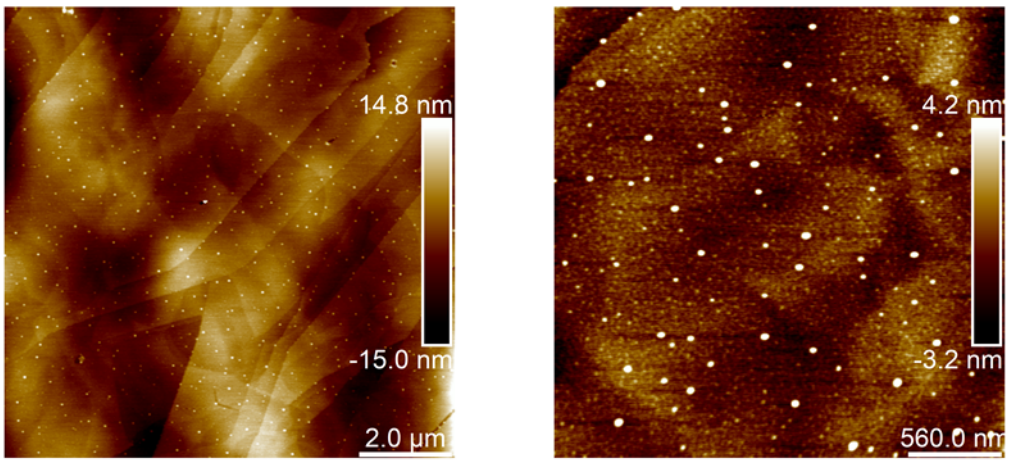

Figure S20: AFM height images of **2-I** prepared by cooling **2** (20 µM, MCH) to 310 K and spin-coating it on HOPG.

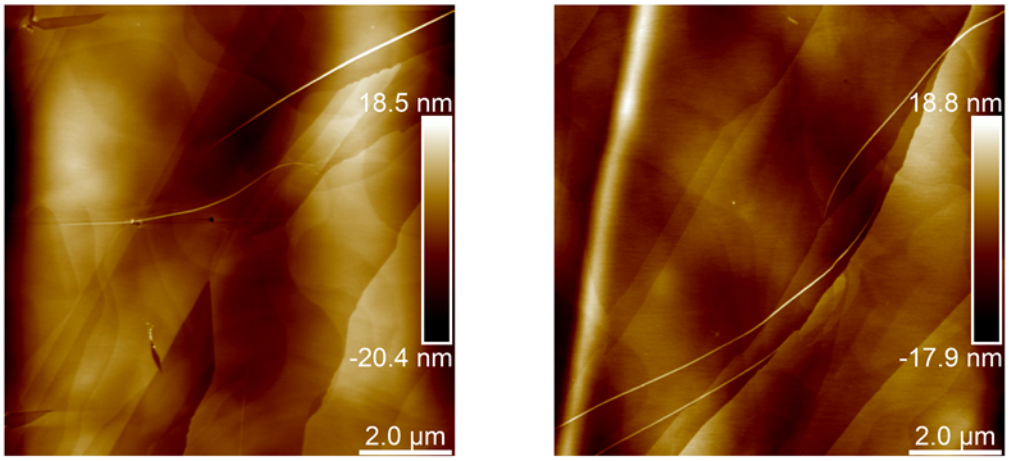

Figure S21: AFM height images of **2-H** prepared by cooling **2** (20 µM, MCH) to 273 K and spin-coating it on HOPG.

X-Ray Crystallography

X-Ray diffraction: Data sets for compound **C** were collected with a Bruker D8 Venture Photon III Diffractometer. Programs used: data collection: *APEX4* Version 2021.4-0[6]; cell refinement: *SAINT* Version 8.40B; data reduction: *SAINT* Version 8.40B; absorption correction, *SADABS* Version 2016/2; structure solution *SHELXT*-Version 2018-3[7]; structure refinement *SHELXL*- Version 2018-3[8]. *R*-values are given for observed reflections, and *w*R^2 values are given for all reflections.

X-ray crystal structure analysis of C (fer10496): A orange, plate-like specimen of $C_{20}H_{20}BFI_2N_2$, approximate dimensions 0.080 mm x 0.160 mm x 0.291 mm, was used for the X-ray crystallographic analysis. The X-ray intensity data were measured on a single crystal diffractometer Bruker D8 Venture Photon III system equipped with a micro focus tube Cu ImS (CuKα, λ = 1.54178 Å) and a MX mirror monochromator. A total of 1033 frames were collected. The total exposure time was 6.85 hours. The frames were integrated with the Bruker SAINT software package using a wide-frame algorithm. The integration of the data using a triclinic unit cell yielded a total of 14719 reflections to a maximum θ angle of 66.57° (0.84 Å resolution), of which 3469 were independent (average redundancy 4.243, completeness = 97.7%, R_{int} = 6.43%, R_{sig} = 5.68%) and 3332 (96.05%) were greater than 2σ(F^2). The final cell constants of a = 7.7147(2) Å, b = 10.7538(3) Å, c = 13.0028(4) Å, α = 96.5190(10)°, β = 105.1110(10)°, γ = 100.9900(10)°, volume = 1007.07(5) Å^3, are based upon the refinement of the XYZ-centroids of 9964 reflections above 20 σ(I) with 7.148° < 2θ < 136.7°. Data were corrected for absorption effects using the Multi-Scan method (SADABS). The ratio of minimum to maximum apparent transmission was 0.458. The calculated minimum and maximum transmission coefficients (based on crystal size) are 0.0530 and 0.2430. The structure was solved and refined using the Bruker SHELXTL Software Package, using the space group *P*-1, with Z = 2 for the formula unit, $C_{20}H_{20}BFI_2N_2$. The final anisotropic full-matrix least-squares refinement on F^2 with 240 variables converged at R1 = 5.41%, for the observed data and wR2 = 14.42% for all data. The goodness-of-fit was 1.075. The largest peak in the final difference electron density synthesis was 3.276 e$^-$/Å^3 and the

largest hole was -1.983 $e^-/Å^3$ with an RMS deviation of 0.251 $e^-/Å^3$. On the basis of the final model, the calculated density was 1.886 g/cm^3 and F(000), 548 e^-. CCDC Nr.: 2386585.

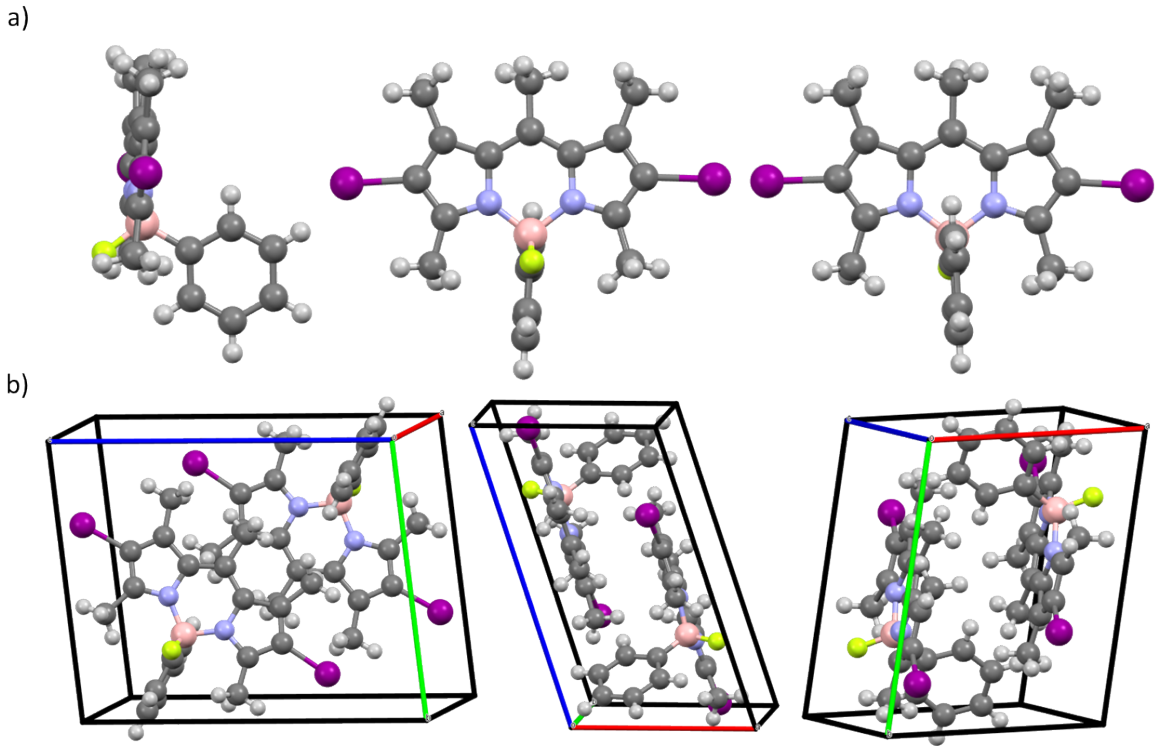

Figure S22: Different views of the X-ray structure of **C**. a) shows different angles of the monomer and b) shows different views of the unit cell.

Orange plate-like crystals of **C** were obtained by slow evaporation of the isolated compound in dichloromethane.

Table S2: Crystal data and refinement details for **C**.

Chemical formula	$C_{20}H_{20}BFI_2N_2$
Formula weight	571.99 g/mol
Temperature	102(2) K
Crystal system	triclinic
Space group	P-1
a	7.7147(2) Å
b	10.7538(3) Å
c	13.0028(4) Å
α	96.5190(10)°
β	105.1110(10)°
γ	100.9900(10)°
Volume	1007.07(5) $Å^3$
Z	2
Density (calculated)	1.886 g/cm^3
Absorption coefficient	24.645 mm^{-1}
Theta range for data collection	3.57 to 66.57°
Reflections collected	14719
Independent reflections	3469 [R(int) = 0.0643]
Coverage of independent reflections	97.7%
Max. and min. transmission	0.2430 and 0.0530
Goodness-of-fit on F^2	1.075
Final R indices	3332 data; $I>2\sigma(I)$ R1 = 0.0541, wR2 = 0.1426
	all data R1 = 0.0549, wR2 = 0.1442
Weighting scheme	$w=1/[\sigma^2(F_o^2)+(0.1078P)^2+0.8775P]$ where $P=(F_o^2+2F_c^2)/3$
Largest diff. peak and hole	3.276 and -1.983 $eÅ^{-3}$
R.M.S. deviation from mean	0.251 $eÅ^{-3}$

Theoretical Calculations

The DFT B3LYP/6-31G(d,p) basis set[9,10] was used to perform the geometry optimization of the different species (monomer, dimers).

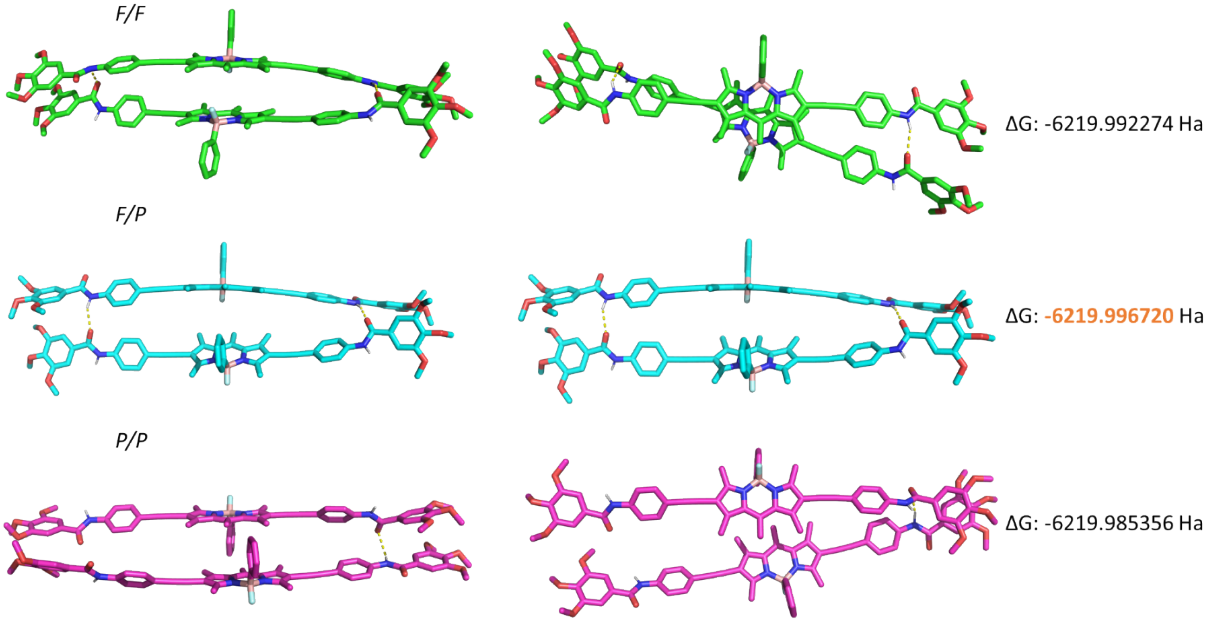

Figure S23: Optimized structures of F/F, F/P and P/P dimers obtained from DFT calculations at the B3LYP/6-31G (d,p) level of theory.

References

[1] A. Rödle; B. Ritschel; C. Mück-Lichtenfeld, V. Stepanenko and G. Fernández, *Chem.–Eur. J.*, 2016, **22**, 15772–15777.

[2] A. Haefele, C. Zedde, P. Retailleau, G. Ulrich and R. Ziessel, *Org. Lett.* 2010, **12**, 1672–1675.

[3] T. W. Hudnall, T.-P. Lin, F. P. Gabbaï *J. Fluor. Chem.* 2010, **131**, 1182–1186.

[4] N. K. Allampally, A. Florian, M. J. Mayoral, C. Rest, V. Stepanenko and G. Fernández, *Chem.-Eur. J.,* 2014, **20**, 10669-10678.

[5] H. M. M. ten Eikelder, A. J. Markvoort, T. F. A. de Greef and P. A. J. Hilbers, An equilibrium model for chiral amplification in supramolecular polymers, *J. Phys. Chem. B*, 2012, **116**, 5291–5301.

[6] Bruker AXS (**2021**) *APEX4 Version 2021.4-0*, *SAINT Version 8.40B* and *SADABS Bruker AXS area detector scaling and absorption correction Version 2016/2*, Bruker AXS Inc., Madison, Wisconsin, USA.

[7] Sheldrick, G. M., *SHELXT – Integrated space-group and crystal-structure determination*, *Acta Cryst.,* **2015**, *A71*, 3-8.

[8] Sheldrick, G.M., *Crystal structure refinement with SHELXL*, *Acta Cryst.*, **2015**, *C71 (1)*, 3-8.

[9] A.D. Becke, *J. Chem. Phys*, 1993, **98**, 5648–5652.

[10] M. M. Francl, W. J. Pietro; W. J. Hehre; J. S. Binkley; M. S. Gordon, D. J. DeFrees, J. A. Pople, *J. Chem. Phys*, 1982, **77**, 3654–3665.